

EQUIVALENT-INCLUSION APPROACH FOR ESTIMATING THE EFFECTIVE ELASTIC MODULI OF MATRIX COMPOSITES WITH ARBITRARY INCLUSION SHAPES USING ARTIFICIAL NEURAL NETWORKS

Nguyen Thi Hai Nhu^a, Tran Anh Binh^{a,*}, Ha Manh Hung^b

^a*Faculty of Information Technology, National University of Civil Engineering,
55 Giai Phong road, Hai Ba Trung district, Hanoi, Vietnam*

^b*Faculty of Building and Industrial Construction, National University of Civil Engineering,
55 Giai Phong road, Hai Ba Trung district, Hanoi, Vietnam*

Article history:

Received 03/12/2019, Revised 07/01/2020, Accepted 07/01/2020

Abstract

The most rigorous effective medium approximations for elastic moduli are elaborated for matrix composites made from an isotropic continuous matrix and isotropic inclusions associated with simple shapes such as circles or spheres. In this paper, we focus specially on the effective elastic moduli of the heterogeneous composites with arbitrary inclusion shapes. The main idea of this paper is to replace those inhomogeneities by simple equivalent circular (spherical) isotropic inclusions with modified elastic moduli. Available simple approximations for the equivalent circular (spherical) inclusion media then can be used to estimate the effective properties of the original medium. The data driven technique is employed to estimate the properties of equivalent inclusions and the Extended Finite Element Method is introduced to modeling complex inclusion shapes. Robustness of the proposed approach is demonstrated through numerical examples with arbitrary inclusion shapes.

Keywords: data driven approach; equivalent inclusion, effective elastic moduli; heterogeneous media; artificial neural network.

[https://doi.org/10.31814/stce.nuce2020-14\(1\)-02](https://doi.org/10.31814/stce.nuce2020-14(1)-02) © 2020 National University of Civil Engineering

1. Introduction

Composite materials often have complex microstructures with arbitrary inclusion shapes and a high-volume fraction of inclusion. Predicting their effective properties from a microscopic description represents a considerable industrial interest. Analytical results are limited due to the complexity of microstructure. Upper and lower bounds on the possible values of the effective properties [1–4] show a large deviation in the case of high contrast matrix-inclusion properties. Numerical homogenization techniques [5–8] determining the effective properties give reliable results but challenge engineers by computational costs, especially in the case of complex three-dimensional microstructure. Engineers prefer practical formulas due to its simplicity [9–13] but practical ones are built from isotropic inclusions of certain simple shapes such as circular or spherical inclusions. In our previous works [14–16]

*Corresponding author. E-mail address: anh-binh.tran@nuce.edu.vn (Binh, T. A.)

proposed an equivalent-inclusion approach that permits to substitute elliptic inhomogeneities by circular inclusions with equivalent properties.

Aiming to reduce the cost of computational homogenization, various methods such as reduced-order models [17], hyper reduction [18], self-consistent clustering analysis [19] have been proposed in the literature. Apart from the mentioned methods, surrogate models have been shown their productivity in many studies such as response surface methodology (RSM) [20] or Kriging [21]. In recent years, data sciences have grown exponentially in the context of artificial intelligence, machine learning, image recognition among many others. Application to mechanical modeling is more recent. Initial applications of the machine learning technique for modeling material can be traced back to the 1990s in the work of [22]. It has pointed out in [22] that the feed-forward artificial neural network can be used to replace a mechanical constitutive model. Various studies have utilized fitting techniques including the artificial neural network (ANN) to build material laws, such as in [23, 24].

In this work, we first attempt to build a model to estimate the effective stiffness matrix of materials for some types of inclusion whose analytical formula maybe not available in the literature, with a small volume fraction using ANNs. Then, we try to define a model to estimate the elastic properties of equivalent circle inclusion. The data in this work is generated by the unit cell method using Extended Finite Element Method (XFEM) which is flexible for the case of complex geometry inclusions. The organization of this paper is as follows. Section 2 briefly reviews the periodic unit cell problem. Section 3 presents the construction of ANN models. Numerical examples are presented in Section 4 and the conclusion is in Section 5.

2. Periodic unit cell problem

In this section, we briefly summarize the unit cell method to estimate the effective elastic moduli of a homogeneous medium with a Representative Volume Element (RVE). The inside domain and its boundary are denoted sequentially as Ω and $\partial\Omega$. The problem defined on the unit cell is as follows: find the displacement field $u(x)$ in Ω (with no dynamics and body forces) such that:

$$\nabla \cdot \sigma(u(x)) = 0 \quad \forall x \quad \text{in} \quad \Omega \quad (1)$$

$$\sigma = \mathbb{C} : \varepsilon \quad (2)$$

where

$$\varepsilon = \nabla \cdot u + \nabla \cdot u^T \quad (3)$$

and verifying

$$\langle \varepsilon \rangle = \bar{\varepsilon} \quad (4)$$

which means that macroscale field equals to the average strain field of the heterogeneous medium. Eq. (1) defines the mechanical equilibrium while Eq. (2) is the Hooke's law. Two cases of boundary condition can be applied to solve Eq. (1) satisfying the equation Eq. (4), which are called as kinematic uniform boundary conditions and periodic boundary condition. The periodic boundary condition, which can generate a converge result with one unit cell, will be used in this work. The boundary conditions can be written as:

$$u(x) = \bar{\varepsilon}x + \tilde{u} \quad (5)$$

where the fluctuation \tilde{u} is periodic on Ω .

The effective elastic tensor is computed according to

$$\mathbb{C}^{eff} = \langle C(x) : A(x) \rangle \quad (6)$$

where $A(x)$ is the fourth order localization tensor relating micro and macroscopic strains such that:

$$A_{ijkl} = \langle \varepsilon_{ij}^{kl}(x) \rangle \quad (7)$$

where $\varepsilon_{ij}^{kl}(x)$ is the strain solution obtained by solving the elastic problem (1) when prescribing a macroscopic strain $\underline{\varepsilon}$ using the boundary conditions with

$$\bar{\varepsilon} = \frac{1}{2} (e_i \otimes e_j + e_j \otimes e_i) \quad (8)$$

In 2D problem, to solve this problem, we solve (1) by prescribing strain as in the following:

$$\bar{\varepsilon}_{11} = \begin{bmatrix} 1 & 0 \\ 0 & 0 \end{bmatrix}; \quad \bar{\varepsilon}_{12} = \begin{bmatrix} 1/2 & 0 \\ 0 & 1/2 \end{bmatrix}; \quad \bar{\varepsilon}_{22} = \begin{bmatrix} 0 & 0 \\ 0 & 1 \end{bmatrix} \quad (9)$$

3. The computation of effective properties and equivalent inclusion coefficients using ANN

Artificial Neural Networks have been inspired from human brain structure. In such model, each neuron is defined as a simple mathematical function. Though some concepts have appeared earlier, the origin of the modern neural network traces back to the work of Warren McCulloch and Walter Pitts [25] who have shown that theoretically, ANN can reproduce any arithmetic and logical function. The idea to determine the equivalent circle inclusions in this work can be seen in Fig. 1.

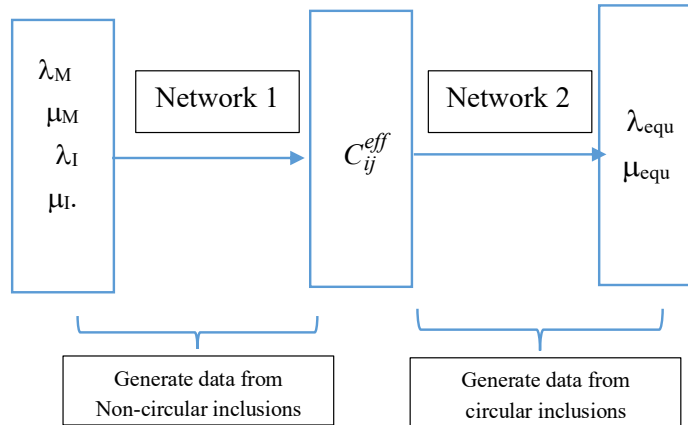


Figure 1. Computation of equivalent inclusion using ANN

Note that, the two networks in Fig. 1 are utilized for the same volume fraction of inclusion. The details of the construction of the two networks will be discussed in the following. The first step, the input fields and output fields of a network are specified. Follow [11], by mapping two formula of an unit cell with a very small volume fraction of inclusion, we first attempt to build an ANN surrogate based on a square unit cell whose inclusion has a volume fraction (\mathbf{f}) of 1% to 5%. To simplify problem, in this work, we keep a constant small \mathbf{f} which is arbitrary chosen. In the two

cases, an ellipse-inclusion (I2) unit cell or a flower-inclusion unit cell (I3), we attempt to extract two components the effective stiffness matrix including C_{11}^{eff} and C_{33}^{eff} by the ANN model from the Lamé constants of the matrix λ_M, μ_M and those of inclusions μ_I, λ_I (see ANN2 and ANN4 in Table 1). For the purpose of finding equivalent parameters, with the circle - inclusion unit cell (I1), the outputs of network are Lamé constants of the inclusion while the input are those of the matrix and the expected C_{11}^{eff} and C_{33}^{eff} of the stiffness matrix. (see ANN1 and ANN3 in Table 1).

Table 1. Information of ANN model

	Case	Volume fraction f	Input	Output	Hidden layers	MSE
ANN1	I1	0.0346	$\lambda_M, \mu_M, C_{11}^{eff}, C_{33}^{eff}$	λ_I, μ_I	15-15	2.2E-3
ANN2	I2	0.0346	$\lambda_M, \mu_M, \lambda_I, \mu_I$	$C_{11}^{eff}, C_{12}^{eff}, C_{33}^{eff}$	15-15	1.0E-6
ANN3	I1	0.0409	$\lambda_M, \mu_M, C_{11}^{eff}, C_{33}^{eff}$	λ_I, μ_I	15-15	3.3E-3
ANN4	I3	0.0409	$\lambda_M, \mu_M, \lambda_I, \mu_I$	$C_{11}^{eff}, C_{21}^{eff}, C_{33}^{eff}$	10-10	1.0E-6

The second step aims to collect data. The calculations are carried out on the unit cell using XFEM. The geometry of these inclusions is described thanks to the following level-set function [26], written as

$$\phi = \left(\frac{x - x_c}{r_x} \right)^{2p} + \left(\frac{y - y_c}{r_y} \right)^{2p} \quad (10)$$

where $r_x = r_y = r_0 + a \cos(b\theta)$; $x = x_c + r_x \cos(b\theta)$; $y = y_c + r_y \cos(\theta)$. For inclusion I3 in Fig. 2(c), we fixed $r_0 = 0.1, p = 6, a = 8, b = 8$. For each case, 5000 data sets were generated using quasi random distribution (Halton-set). The data is divided into 3 parts including 70% for training, 15% for validation and 15% for validating. Note that, the surrogate model just works for interpolation problem, so the input must be in a range of value. In this work, the bound is selected randomly. The upper bound of inputs (see Fig. 1) are [20.4984 2.0000 50.4937 20.4975] and the lower bound of inputs are [0.5017 0.0001 0.5027 0.5011].

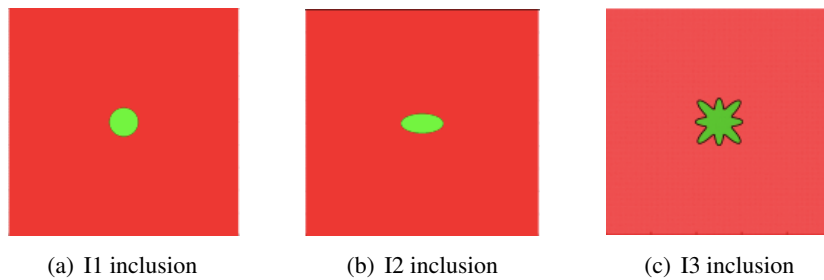


Figure 2. Three types of unit cell

The third step works on the architecture of the surrogate model. This step includes determining the number of layers and neurons, the activation function, the lost function. In the following, we employ the Mean square error (MSE) as the lost function. For the activation function, tang-sigmoid, which is popular and effective for many regression problems, will be utilized:

$$f(x) = \frac{e^x - e^{-x}}{e^x + e^{-x}} - 1 \quad (11)$$

The input data was then normalized using Max-min-scaler, written as:

$$x = 2 \frac{x - x_{\min}}{x_{\min} + x_{\max}} - 1 \quad (12)$$

The fourth step selects a training algorithm. Various algorithm is available in literature, however, the most effective one is unknown before the training process is conducted. Some are available in Matlab are Lavenberg-Marquardt, Bayesian Regularization, Genetic Algorithm. One may combine several algorithms to obtain the expected model. Evaluating each algorithm or network architecture is out of scope of this work. All ANN networks here in were trained by the popular Lavenberg-Marquardt algorithm.

The fifth step is to train the network: use the constructed data to fit the different parameters and weighting functions in the ANN. Various factors can affect the training time which can be defined by the trainer. In case the expected performance is obtained, the training process is stopped, and the result will be employed. In contrast, when the performance does not reach the expectation, another training process may be conducted with a change in the parameters (e.g. the number of echoes, the minimum gradient, the learning rate in gradient-based training algorithm ...).

After the sixth step, which aims to analyze the performance, we use the network. Note that the application of network is limited by the input range which has been chosen before training.

4. Numerical results

4.1. Computation of the effective stiffness matrix C^{eff} using surrogate models for periodic unit cell problem

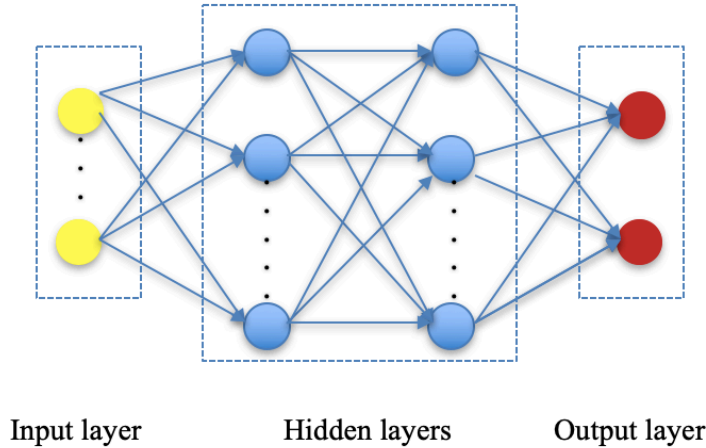


Figure 3. A multilayer perceptron. The details for each ANN models are depicted in Table 1

This section shows some information of the trained networks which will be used for the problem in Section 4.2 and 4.3. We compare the results generated by trained ANNs and XFEM method. Specifically, we used ANN2 and ANN4 for I2 and I3, respectively. As discussed in Section 3.4, we fix \mathbf{f} and vary the elastic constant. The agreement of ANN models and the unit cell method using XFEM is depicted in Fig. 4 and Fig. 5, which show that the surrogate models are reliable. Note that, we don't

attempt to use any type of realistic materials and the problem is plain strain. In the relation with the two Lamé constants, the material stiffness matrix is written as:

$$C = \begin{bmatrix} \lambda + 2\mu & 2\lambda & 0 \\ 2\lambda & 2\mu & 0 \\ 0 & 0 & \mu \end{bmatrix} \quad (13)$$

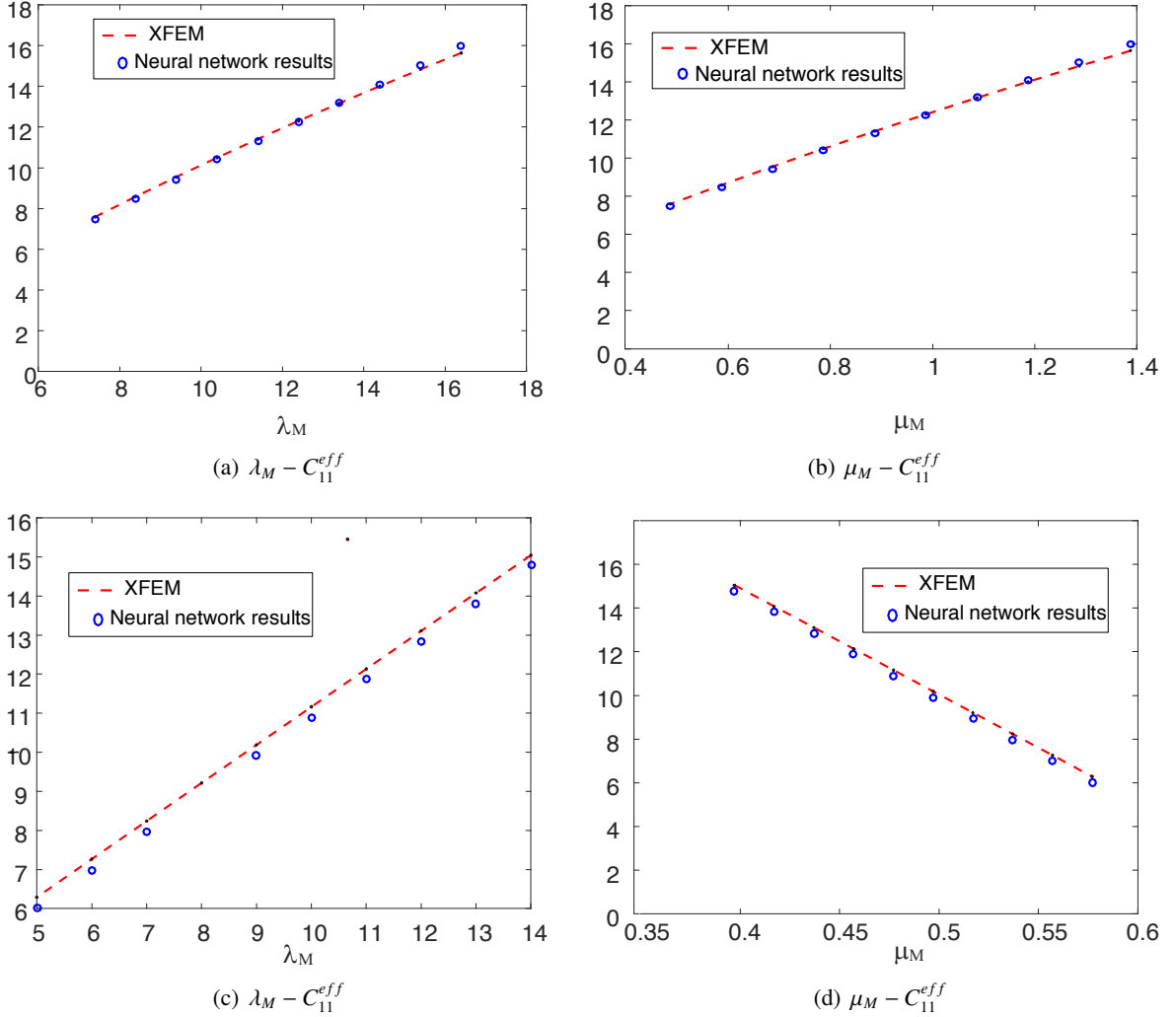


Figure 4. Comparison of results (C_{11}^{eff} components) of ANN2 and XFEM (periodic unit cell problem) for case I2

In Figs. 4(a) and 4(b): λ_M decreases from 16 to 7 while μ_M decrease from 1.3870 to 0.4870 simultaneously and respectively, (λ_I, μ_I) are constant at (0.5058, 0.5023); In Figs. 4(c) and 4(d): λ_M decreases from 14 to 5 while μ_M increase from 0.3971 to 0.5771. (λ_I, μ_I) are fixed at (44.1500, 14.9600) for all the cases.

In Figs. 5(a) and 5(b): λ_M increases from 17.3918 to 8.3918 while μ_M increases from 1.4670 to 1.2870 simultaneously and respectively. In Figs. 5(c) and 5(d): λ_M decreases from 16 to 7 while ν_M

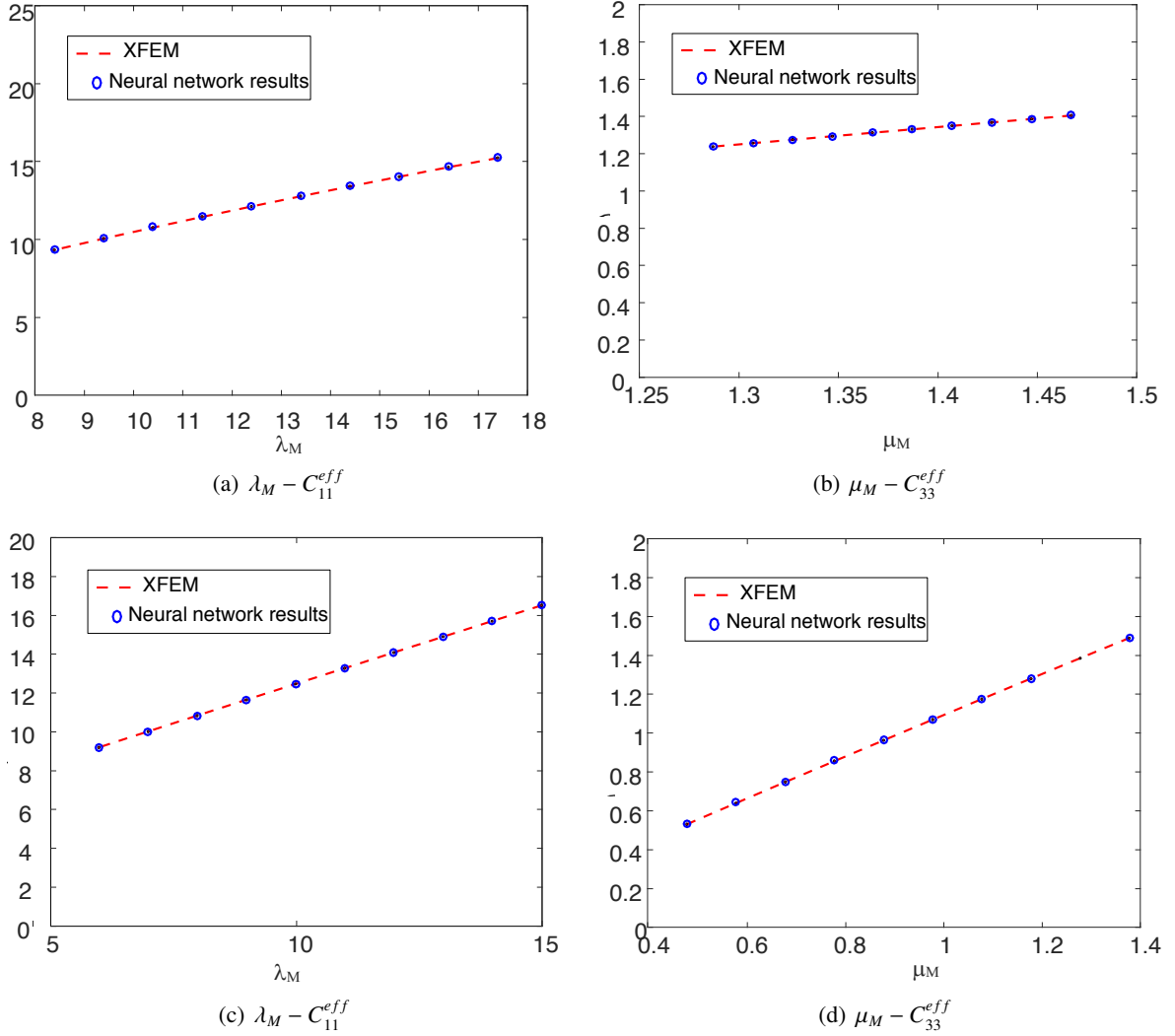


Figure 5. Comparison of results (C_{11}^{eff} and C_{33}^{eff} components) of ANN4 and XFEM for case I3

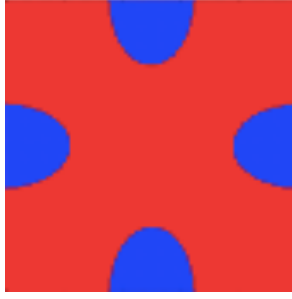
decreases from 1.3870 to 0.4870 simultaneously and respectively. In both all the cases, (λ_I, μ_I) are fixed at (0.5058, 0.5023).

4.2. Computation of C equivalent inclusion of I2 (ellipse inclusion)

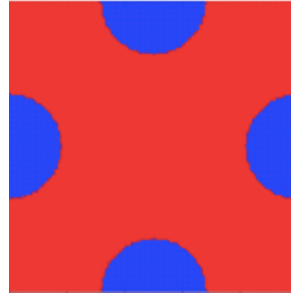
We aim to find λ_{equ}, μ_{equ} of the circle equivalent inclusion (I1), which has the same volume fraction with other type of inclusion (case I2, I3 in this work). To compute these coefficients, we combine two networks as shown in Fig. 1: ANN1 for Network1 and the ANN2 for Network 2.

Three tests will be computed to validate the surrogate models: In Test 1 (Fig. 6), the sample has the size of $1 \times 1 \text{ mm}^2$ and contains 4 halves of an ellipse inclusion; in Test 2 (Fig. 7), the sample has the size of $1 \times 1.73 \text{ mm}^2$ in which inclusions distribute hexagonally and Test 3 (Fig. 8) which contains 100 random inclusions

In these tests, we consider two sets of data. Assuming that $\lambda_M, \mu_M, \lambda_I, \mu_I$ are known, we choose a small volume fraction and using ANN1 to generate the input for ANN2. Two data sets are examined:

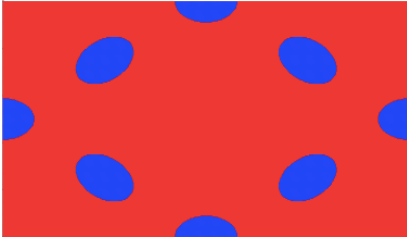


(a) A sample with 4 halves of ellipse inclusions

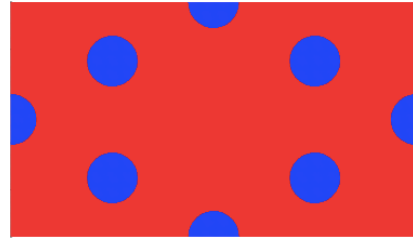


(b) The equivalent medium of the sample in Fig. 6(a)

Figure 6. Test 1: The sample in (a) has the size of $1 \times 1 \text{ mm}^2$ and the ratio between radius of $a/b = 1.5$

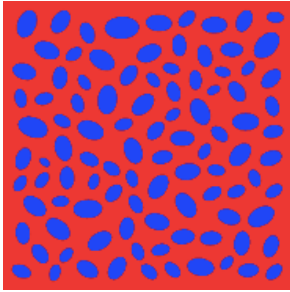


(a) A sample with 4 and $4 \times 1/2$ ellipse inclusions

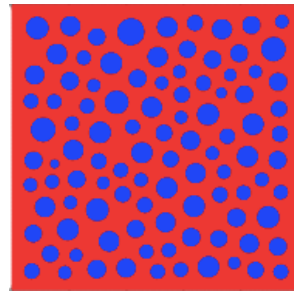


(b) The equivalent medium of the sample in Fig. 7(a)

Figure 7. Test 2: a rectangular sample has the size of $1 \times 1.73 \text{ mm}^2$ (a) and its equivalent medium (b)



(a) A sample with 100 ellipse inclusions



(b) The equivalent medium of the sample in Fig. 8(a)

Figure 8. Test 3: A sample with 100 random ellipse inclusions (a) and its equivalent medium with 100 circular inclusions (b)

- Dataset 1: $\lambda_M = 17.3918 \text{ N/mm}^2$; $\lambda_I = 0.5058 \text{ N/mm}^2$, $\mu_M = 1.4870 \text{ N/mm}^2$, $\mu_I = 0.5023 \text{ N/mm}^2$, and $\lambda_{equ} = 0.3822 \text{ N/mm}^2$, $\mu_{equ} = 1.4528 \text{ N/mm}^2$.

- Dataset 2: $\lambda_M = 18.7749 \text{ N/mm}^2$; $\lambda_I = 40.2908 \text{ N/mm}^2$, $\mu_M = 0.4822 \text{ N/mm}^2$, $\mu_I = 16.4163 \text{ N/mm}^2$, and $\lambda_{equ} = 39.9912 \text{ N/mm}^2$, $\mu_{equ} = 16.2965 \text{ N/mm}^2$.

Figs. 9–11 compare the effective properties of the two media in Test 1, Test 2, Test 3 respectively. We can see that with the equivalent properties of inclusions, equivalent media reflect very well it referenced media.

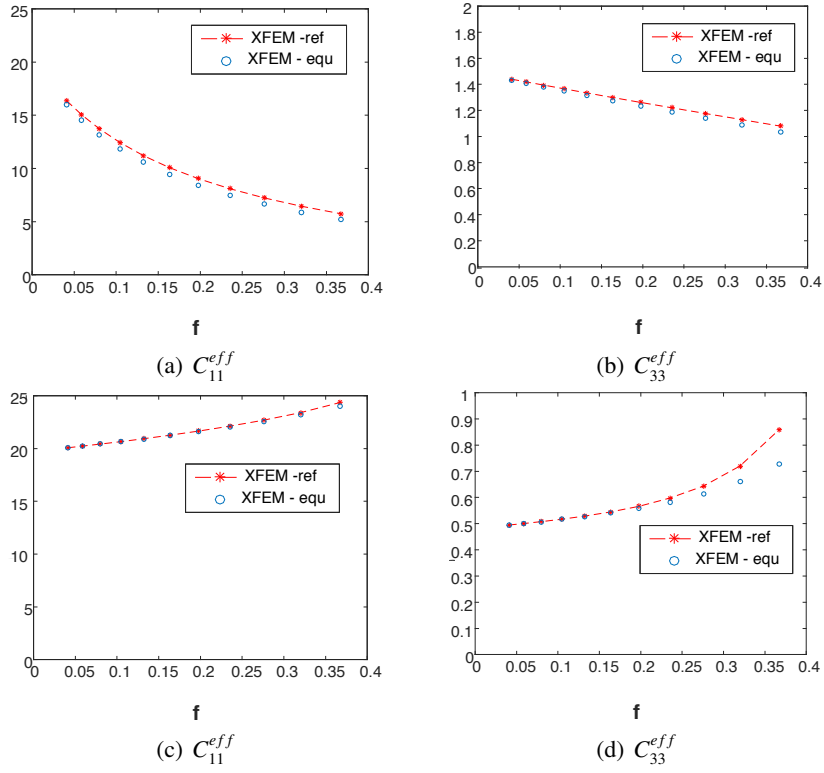


Figure 9. Comparison of C_{11}^{eff} and C_{33}^{eff} in Test 1 (Fig. 6): using Data set 1 (a, b) and Data set 2 (c, d)

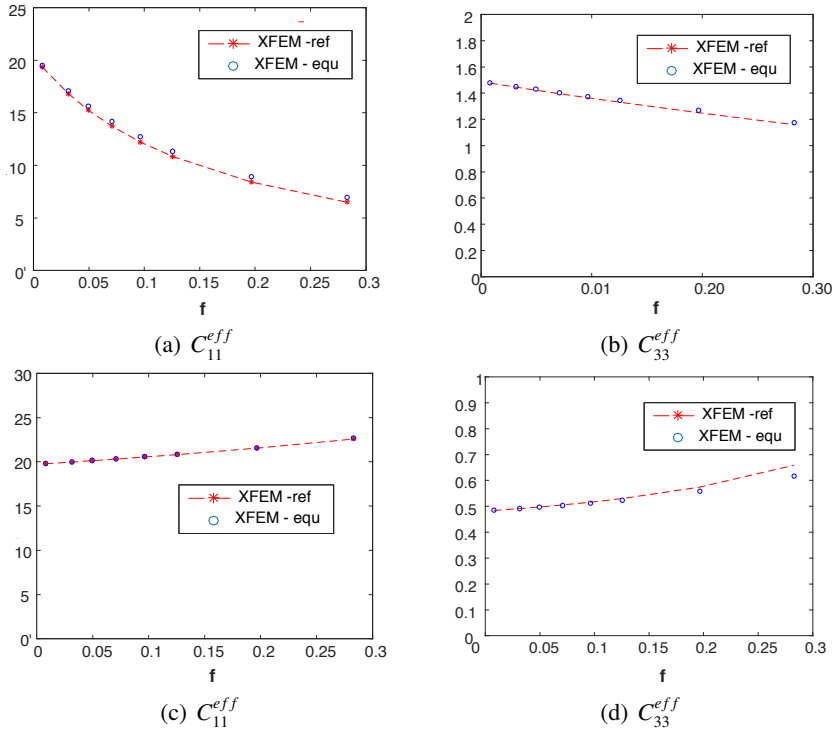


Figure 10. Comparison of C_{11}^{eff} and C_{33}^{eff} in Test 2 (Fig. 7): using Data set 1 (a, b) and Data set 2 (c, d)

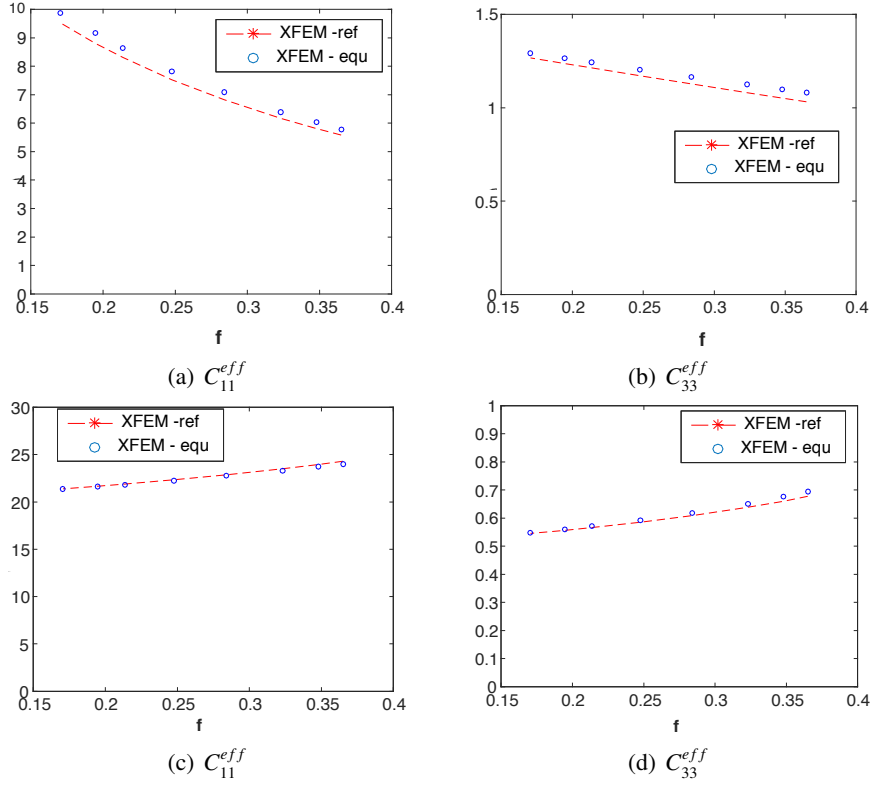


Figure 11. Comparison of C_{11}^{eff} and C_{33}^{eff} in Test 3 (Fig. 8): using Data set 1 (a, b) and Data set 2 (c, d).

4.3. Computation of C equivalent inclusion of I3 (flower inclusion)

Similar to the case I2, we employ ANN3 and ANN4 (for Network 1 and Network 2 in Fig. 1, respectively) to generate the equivalent parameter for circle inclusion. As the geometry of flower inclusion is quite complicated, we reduce the input dimension by exclude the properties of matrix. Specifically, the network is for the case $\lambda_M = 17.3918 \text{ N/mm}^2$, $\mu_M = 1.4870 \text{ N/mm}^2$. The data of inclusion $\lambda_I = 0.5058 \text{ N/mm}^2$, $\mu_I = 0.5023 \text{ N/mm}^2$ and the equivalent inclusion computed by ANNs includes $\lambda_{equ} = 0.3872 \text{ N/mm}^2$, $\mu_{equ} = 0.4547 \text{ N/mm}^2$. These results are then validated in the two following tests which have the same size of $1 \times 1 \text{ mm}^2$ (see Figs. 12(a) and 12(b)).

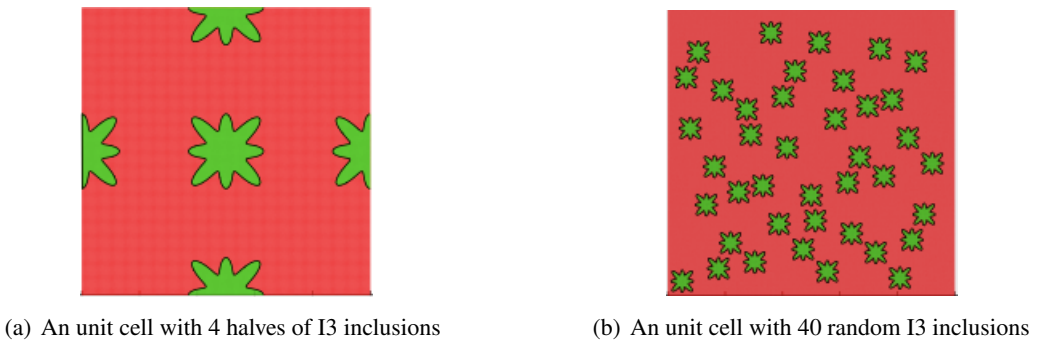


Figure 12. Two unit cells of the size $1 \times 1 \text{ mm}^2$

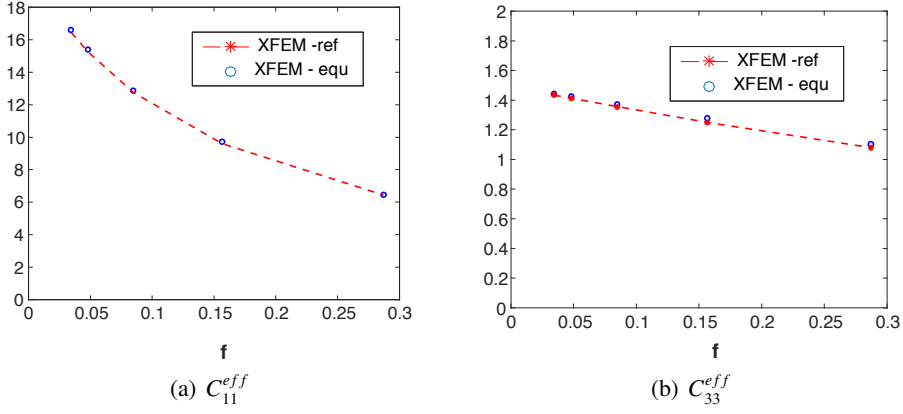


Figure 13. Comparison of C_{11}^{eff} (a) and C_{33}^{eff} (b) for Test 4 (Fig. 12(a)): the result computed using equivalent inclusion (XFEM-eq) shows a good match with the reference result (XFEM-ref)

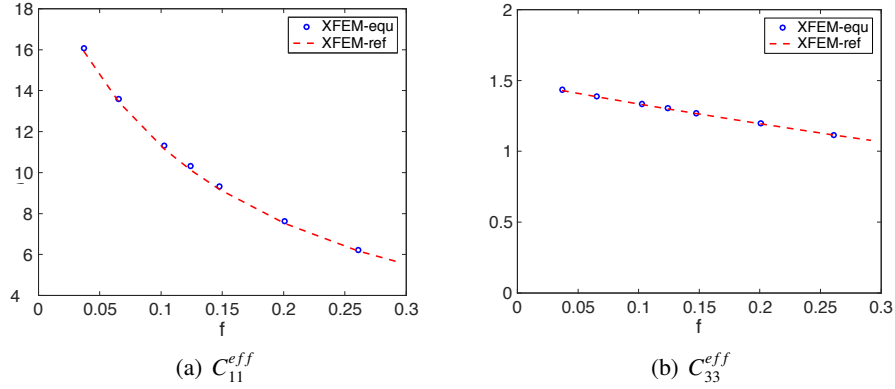


Figure 14. Comparison of C_{11}^{eff} (a) and C_{33}^{eff} (b) for Test 4 (Fig. 12(b)): the result computed using equivalent inclusion (XFEM-eq) shows a good match with the reference result (XFEM-ref)

The results compared in Figs. 13 and 14 again show a good match between the two media, which suggests the reliability of the proposed approach.

5. Conclusions

In this paper, we have presented a novel approach for estimating the equivalent circular inclusion. We've shown the capacity of the ANN surrogate for the unit cell method to compute the effective stiffness matrix in some cases of inclusion with a small specified volume fraction. Using a second network, which interpolates properties of the circular inclusion from the expected effective stiffness matrix, we have proposed a new approach to deal with the equivalent inclusion problem by combining two ANN models. The proposed approach allows us to apply for the case when an analytic formula to compute effective elastic moduli is not available, eg. I3 in this work. The results in section 4 show a good agreement between the equivalent medium and the referenced medium, which reveals the potential of data driven approach for this problem. For future works, we'll try to improve the quality of the network and apply for various types of inclusions.

Acknowledgements

This research is funded by Vietnam National Foundation for Science and Technology Development (NAFOSTED) under Grant Number 107.02-2017.309.

References

- [1] Hashin, Z., Shtrikman, S. (1962). A variational approach to the theory of the effective magnetic permeability of multiphase materials. *Journal of Applied Physics*, 33(10):3125–3131.
- [2] Miller, M. N. (1969). [Bounds for effective electrical, thermal, and magnetic properties of heterogeneous materials](#). *Journal of Mathematical Physics*, 10(11):1988–2004.
- [3] Phan-Thien, N., Milton, G. W. (1982). [New bounds on the effective thermal conductivity of N-phase materials](#). *Proceedings of the Royal Society of London. A. Mathematical and Physical Sciences*, 380 (1779):333–348.
- [4] Chinh, P. D. (2011). [Bounds on the effective conductivity of statistically isotropic multicomponent materials and random cell polycrystals](#). *Journal of the Mechanics and Physics of Solids*, 59(3):497–510.
- [5] Dunant, C. F., Bary, B., Giorla, A. B., Péniguel, C., Sanahuja, J., Toulemonde, C., Tran, A.-B., Willot, F., Yvonnet, J. (2013). [A critical comparison of several numerical methods for computing effective properties of highly heterogeneous materials](#). *Advances in Engineering Software*, 58:1–12.
- [6] Tran, A. B., Yvonnet, J., He, Q.-C., Toulemonde, C., Sanahuja, J. (2011). [A multiple level set approach to prevent numerical artefacts in complex microstructures with nearby inclusions within XFEM](#). *International Journal for Numerical Methods in Engineering*, 85(11):1436–1459.
- [7] Moulinec, H. (1994). A fast numerical method for computing the linear and nonlinear mechanical properties of composites. *Comptes Rendus Mecanique*, 318:1417–1423.
- [8] Michel, J. C., Moulinec, H., Suquet, P. (2001). [A computational scheme for linear and non-linear composites with arbitrary phase contrast](#). *International Journal for Numerical Methods in Engineering*, 52 (1-2):139–160.
- [9] Pham, D. C., Tran, N. Q., Tran, A. B. (2017). [Polarization approximations for elastic moduli of isotropic multicomponent materials](#). *Journal of Mechanics of Materials and Structures*, 12(4):391–406.
- [10] Pham, D. C., Tran, A. B., Do, Q. H. (2013). [On the effective medium approximations for the properties of isotropic multicomponent matrix-based composites](#). *International Journal of Engineering Science*, 68: 75–85.
- [11] Tran, A. B., Pham, D. C. (2015). [Polarization approximations for the macroscopic elastic constants of transversely isotropic multicomponent unidirectional fiber composites](#). *Journal of Composite Materials*, 49(30):3765–3780.
- [12] Norris, A. N., Callegari, A. J., Sheng, P. (1985). [A generalized differential effective medium theory](#). *Journal of the Mechanics and Physics of Solids*, 33(6):525–543.
- [13] Milgrom, M., Shtrikman, S. (1989). [A layered-shell model of isotropic composites and exact expressions for the effective properties](#). *Journal of Applied Physics*, 66(8):3429–3436.
- [14] Quyet, T. N., Chinh, P. D., Binh, T. A. (2015). Equivalent-inclusion approach for estimating the elastic moduli of matrix composites with non-circular inclusions. *Vietnam Journal of Mechanics*, 37(2):123–132.
- [15] Do, Q. H., Tran, A. B., Pham, D. C. (2016). [Equivalent inclusion approach and effective medium approximations for the effective conductivity of isotropic multicomponent materials](#). *Acta Mechanica*, 227(2): 387–398.
- [16] Chinh, P. D., Binh, T. A. (2016). Equivalent-inclusion approach for the conductivity of isotropic matrix composites with anisotropic inclusions. *Vietnam Journal of Mechanics*, 38(4):239–248.
- [17] Hernández, J. A., Oliver, J., Huespe, A. E., Caicedo, M. A., Cante, J. C. (2014). [High-performance model reduction techniques in computational multiscale homogenization](#). *Computer Methods in Applied Mechanics and Engineering*, 276:149–189.

- [18] Zahr, M. J., Avery, P., Farhat, C. (2017). [A multilevel projection-based model order reduction framework for nonlinear dynamic multiscale problems in structural and solid mechanics](#). *International Journal for Numerical Methods in Engineering*, 112(8):855–881.
- [19] Bessa, M. A., Bostanabad, R., Liu, Z., Hu, A., Apley, D. W., Brinson, C., Chen, W., Liu, W. K. (2017). [A framework for data-driven analysis of materials under uncertainty: Countering the curse of dimensionality](#). *Computer Methods in Applied Mechanics and Engineering*, 320:633–667.
- [20] Myers, R. H. (1999). [Response surface methodology—current status and future directions](#). *Journal of Quality Technology*, 31(1):30–44.
- [21] Simpson, T. W., Mauery, T. M., Korte, J. J., Mistree, F. (2001). [Kriging models for global approximation in simulation-based multidisciplinary design optimization](#). *AIAA Journal*, 39(12):2233–2241.
- [22] Ghaboussi, J., Garrett Jr, J. H., Wu, X. (1991). [Knowledge-based modeling of material behavior with neural networks](#). *Journal of Engineering Mechanics*, 117(1):132–153.
- [23] Yvonnet, J., He, Q.-C. (2007). [The reduced model multiscale method \(R3M\) for the non-linear homogenization of hyperelastic media at finite strains](#). *Journal of Computational Physics*, 223(1):341–368.
- [24] Le, B. A., Yvonnet, J., He, Q.-C. (2015). [Computational homogenization of nonlinear elastic materials using neural networks](#). *International Journal for Numerical Methods in Engineering*, 104(12):1061–1084.
- [25] McCulloch, W. S., Pitts, W. (1943). [A logical calculus of the ideas immanent in nervous activity](#). *The Bulletin of Mathematical Biophysics*, 5(4):115–133.
- [26] Yvonnet, J., Quang, H. L., He, Q. C. (2008). [An XFEM/level set approach to modelling surface/interface effects and to computing the size-dependent effective properties of nanocomposites](#). *Computational Mechanics*, 42(1):119–131.